Instantaneous complex spectral domain OCT using 3x3 fiber couplers

Marinko V. Sarunic, Michael A. Choma, Changhuei Yang, Joseph A. Izatt

Marinko V. Sarunic, Michael A. Choma, Changhuei Yang, Joseph A. Izatt, "Instantaneous complex spectral domain OCT using 3x3 fiber couplers," Proc. SPIE 5316, Coherence Domain Optical Methods and Optical Coherence Tomography in Biomedicine VIII, (1 July 2004); doi: 10.1117/12.531422

SPIE.

Event: Biomedical Optics 2004, 2004, San Jose, CA, United States

Instantaneous complex spectral domain OCT using 3x3 fiber couplers

Marinko V. Sarunic, Michael A. Choma, Changhuei Yang, Joseph A. Izatt

Department of Biomedical Engineering, Duke University, Durham, NC 27708

ABSTRACT

We report that the complex conjugate ambiguity in spectral domain OCT approaches (including swept source OCT and Fourier-domain OCT) may be removed by the use of novel interferometer designs based on NxN couplers. An interferometer based on a 3x3 truly fused fiber coupler with equal splitting ratios provides simultaneous access to components of the complex interferometric signal separated by 120°. These phase components may be converted to quadrature components by use of a simple trigonometric operation, and then inverse Fourier transformed to obtain A-scans and images free of complex conjugate artifact. We demonstrate instantaneous complex spectral-domain OCT using a novel Fourier-domain OCT system employing photodiode arrays, and will also report on a similar system design for instantaneous complex swept-source OCT.

Keywords: spectral domain optical coherence tomography

1. INTRODUCTION

Interferometry with broadband light sources has become a widely used technique for imaging in biological samples using optical coherence tomography (OCT). Very recently, some investigators [1,2] have suggested that spectral domain OCT (SDOCT) techniques such as swept-source OCT (SSOCT) [3] and Fourier-Domain OCT (FDOCT) [4] have significant advantages both in sensitivity and robustness over the widely used approach of time-domain OCT (TDOCT). In SDOCT, the positions of scatterers in a sample are resolved by acquiring the optical spectrum of sample light interfered with light from a single, stationary (or phase stepped), reference reflector. In SSOCT, the spectrum is acquired in a single detector by temporally sweeping the source spectrum, while in FDOCT the spectrum is acquired by dispersing interference light from a broadband source across a detector array. For the discussion below, consider the Michelson type fiber interferometer illustrated in Fig. 1.

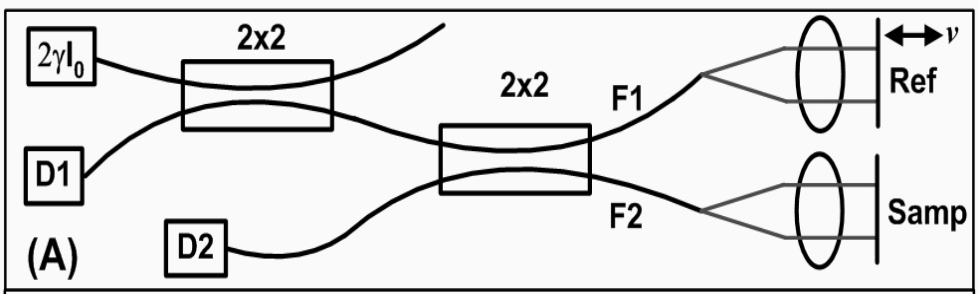

Figure 1. Fiber based Michelson interferometer. For SSOCT, the elements D_1 ad D_2 are photodiodes which are sampled simultaneously, whereas in FDOCT D1 and D2 represent detectors at the output of spectrometers.

Coherence Domain Optical Methods and Optical Coherence Tomography in Biomedicine VIII, edited by Valery V. Tuchin, Joseph A. Izatt, James G. Fujimoto, Proc. of SPIE Vol. 5316 (SPIE, Bellingham, WA, 2004) · 1605-7422/04/$15 · doi: 10.1117/12.531422

In either SSOCT or FDOCT, the total electric field at the detector is related to

$$E_{net\,i}[k_m] = \frac{1}{2^i}\frac{t}{e}\rho\left(\sqrt{R_R}E[k_m]e^{j(2x_1k_m)} + \sqrt{R_S}E[k_m]e^{j(2x_2k_m+\varphi_i)}\right)$$
$$D_i[k_m] = \frac{1}{2^i}\frac{t}{e}\rho\cdot S[k_m]\cdot\left[R_R + R_S + 2\sqrt{R_R R_S}\cos(2\Delta x k_m + \varphi_i)\right], \quad (1)$$

where $E[k_m]$ and $S[k_m]$ are the wavenumber indexed electric field amplitude and intensity, respectively, and $E_{net\,i}[k_m]$ is the net electric field intensity and $D_i[k_m]$ is the intensity at the i^{th} detector, R_S and R_R are the sample and reference reflectivities, respectively, φ_i is the phase shift associated with the i^{th} detector signal, and $D_i[k_m]$ has units watts per wavenumber. The detector responsivity accounted for in ρ and the detector elements are indexed by $m\in\{1,M\}$, where M is the number of pixels on the detector for FDOCT and the number of bandwidth elements sampled in SSOCT. The double-pass position of each sample reflection is encoded in the frequency of cosinusoidal variations of $D_i[k_m]$, while the sample reflectivity is encoded in the visibility of these variations. The spectrally indexed detector outputs therefore represent the real part of the discrete Fourier transform of an OCT A-scan given by

$$D_i[x_n] = \sum_{m=1}^{M} D_i[k_m]e^{-(j2\pi(2k_m x_n))}. \quad (2)$$

The factor of 2 in the kernel exponent ensures the recovery of single-sided distances, and $n\in\{1,M\}$. In the x-domain, the channel spacing is $\delta x=1/\Delta k$ and the scan depth is $\Delta x_{max}=1/\delta k$ [$-1/(2\delta k)$ to $+1/(2\delta k)$]. However, because the A-scan is symmetric (as will be discussed below) the effective scan depth is $\Delta x_{max}=1/(2\delta k)$.

Qualitatively, Eq. (2) has three peaks for the case of a single reflector in the sample arm with path length difference of Δx. The central peak is located at x=0, this is the DC component due to the transform of the source spectrum $S[k_m]$. The two other peaks are symmetric, located at $x_n=\pm\Delta x$, and are due to the interferometric portion of Eq. (2). The symmetric peaks arise as an artifact of the Fourier transform. Since photodiode and CCD cameras only measure the intensity, the phase information of the field is lost. As result, the signal detected is purely real valued, and the Fourier transform of the signal is therefore complex conjugate symmetric. The consequence of the complex conjugate symmetry of the A-scan is that a reflection at $+\Delta x$ cannot be distinguished from a reflector at $-\Delta x$, and thus samples containing reflections at both $+\Delta x$ and $-\Delta x$ contain significant artifacts which cannot be removed by post-processing. This property of SDOCT techniques is referred to as the complex conjugate ambiguity. The complex conjugate ambiguity can be resolved by additionally collecting the imaginary part of the complex interferometric signal described in Eq. (1b). Since sine and cosine are related by a phase shift of $\pi/2$, recording a spectrum corresponding to a displacement of $2\Delta x$ by a value of $\lambda/2$ recovers the full complex signal [4]. The complete complex signal can then be written as

$$D_i[k_m] = D_i^0[k_m] + jD_i^{90}[k_m], \quad (3)$$

where the superscript notation represents the 0^o and 90^o phase separated measurements. The Fourier transform of the full complex signal is thus an A-scan with the positive or negative path length difference of the sample arm reflector unambiguously determined

In order to remove the DC artifact, a third spectrum representing the spectral shape of the source must also be acquired. In the limit that the reference arm power is much higher than the sample arm power, a reference DC spectrum can be acquired by collecting light from the reference arm only (sample arm blocked). Alternately, when many Ascans are available, as when acquiring a Bscan, the DC spectrum can be obtaining by averaging over all the spectra, exploiting the fact that the net contribution of the interference infringes must sum to zero. With the DC spectrum acquired by either technique, the complex signal with DC component removed is given by:

$$D_i[k_m] = \left(D_i^0[k_m] - D_i^{DC}[k_m]\right) + j\left(D_i^{90}[k_m] - D_i^{DC}[k_m]\right), \tag{4}$$

where the $D^{DC}[k_m]$ term represents the source spectrum indexed by wavenenumber.

In previous implementations of FDOCT, phase shifting interferometry techniques have been exploited to dither the phase of the reference electric field in order to collect real and imaginary parts on sequential scans [4]. Phase shifting, however, requires a stable and carefully calibrated reference arm step, is not instantaneous, and is sensitive to interferometer drift between phase-shifted acquisitions. To the best of our knowledge, phase shifting for resolution of the complex conjugate ambiguity has not yet been attempted in SSOCT, although the benefits and drawbacks of this approach will be similar as for FDOCT.

A potentially more elegant solution for complex signal acquisition in SDOCT consists of making use of the intrinsic, wavelength-independent, non-complementary phase relationships which exist between light returning from interferometers constructed from higher order (NxN) fiber couplers [5]. For example, a Michelson-type interferometer constructed using a truly fused 3x3 coupler having an even split ratio between the ports ideally exhibits a phase delay between input ports of 120^o [6]. Other phase delays (including 90^o) may be obtained in 3x3 couplers with non-even splitting ratios, or by use of couplers with higher port counts [5]. Thus, a very robust complex FDOCT system can be constructed from a 3x3 coupler as illustrated in Fig. 2 to simultaneously acquire multiple phase components of the complex interferometric signal. A similar approach leads to an analogous interferometer design for instantaneous complex SSOCT.

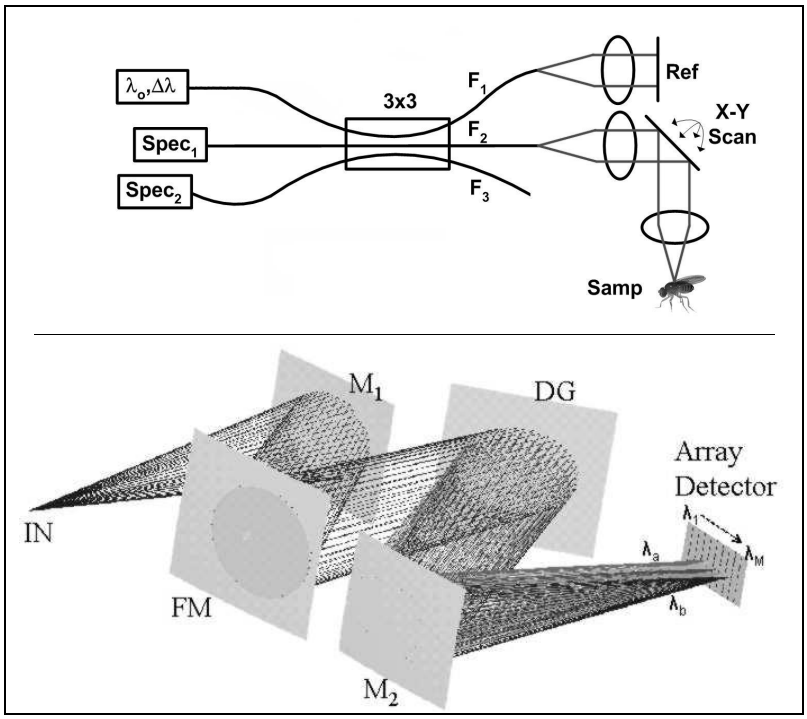

Figure 2. Fourier domain OCT system employing a 3x3 truly fused fiber coupler. Each $Spec_n$ represents a spectrometer with an array detector. For a 3x3 coupler with equal splitting ratios between outputs F_n, the interferometric signal on the spectrometers is separated in phase by 120^o. The low coherence source has a center wavelength λ_o and a FWHM of $\Delta\lambda$. F = fiber; Samp = sample; ref = reference mirror. b) Czerny-Turner spectrometer configuration (Thermo-Oriel). Mirror M_1 collimates input light onto diffraction grating (DG) while mirror M_2 addresses the dispersed wavelengths onto a 1024 element photodiode array detector. (IN: input, FM: off axis spherical fold mirror.)

The phase spectra collected by spectrometers 1 and 2 in Fig. 2 may be converted to quadrature components (0^o and 90^o) using a simple trigonometric relationship, assuming the exact splitting ratios of the coupler are known (they can be readily measured). Defining one of the acquired spectra as the real part of the complex signal $i_n=i_{Re}$, the imaginary part i_{Im} is obtained from the cosine sum rule, as [5]:

$$i_{Im} = \frac{i_n \cos(\Delta\phi_{mn}) - \beta_{mn}\, i_m}{\sin(\Delta\phi_{mn})}. \tag{5}$$

Here, $\Delta\phi_{mn} = \phi_m - \phi_n$ is the phase difference, and β_{mn} the wavelength dependent power splitting ratio between output ports m and n of the coupler. Both $\Delta\phi_{mn}$ and β_{mn} are functions of the coupling coefficients α_{ab} from fiber *a* to fiber *b*. The derived quadrature spectra are separated in phase by 90^o, thus the inverse Fourier transform of the full complex signal $i_{Re} + j \cdot i_{Im}$ reveals the depth-reflectivity profile of the sample with the complex conjugate ambiguity resolved.

2. METHODS

We constructed the instantaneous complex FDOCT setup illustrated in Fig. 2 using a superluminescent diode source (Superlum; λ_o=830nm, $\Delta\lambda$=28nm), an AC Photonics, Inc. 3x3 truly fused fiber coupler, and two spectrometers (Thermo-Oriel, 1/8m focal length) with 1024 element photodiode array detectors (Hamamatsu, 2.5mm tall elements on a 25μm pitch). The power incident on the sample was 1mW, and the line rate was 500Hz. For the complex conjugate resolved Ascans, the effective maximum full depth is equal to ~800um by the Nyquist sampling criteria for this system. The coupling coefficients measured are shown in Figure 3, as well as the derived values of $\Delta\phi_{mn}$ and β_{mn} used for the conversion to quadrature.

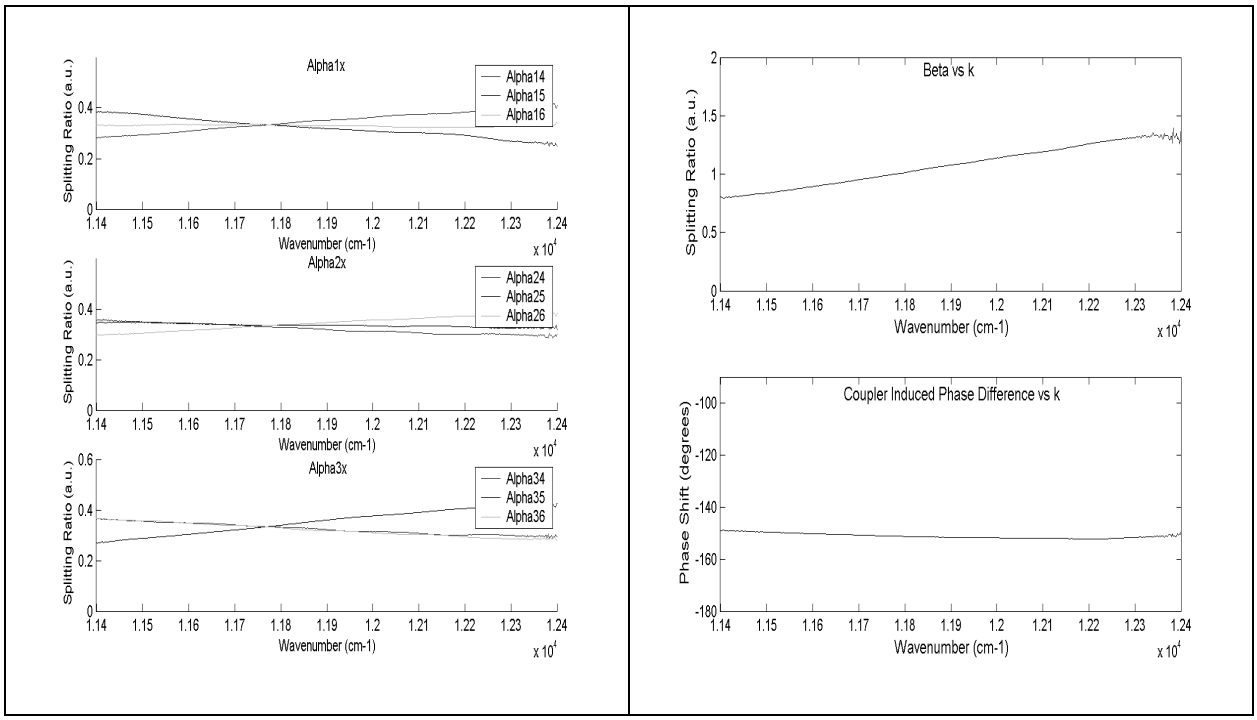

Figure 3. a) Coupling coefficients measured as a function of wavenumber for the 3x3 coupler used. b) The derived curves for β and $\Delta\phi$ from the coupling coefficients.

3. RESULTS

The quality of the quadrature conversion can be quantified by comparing the complex conjugate resolved Ascan with an unresolved Ascan. For this comparison, a mirror attenuated by a 2.5OD neutral density filter was placed in the sample arm. For both sets of data, the DC component was subtracted by measuring the reference arm power only with the sample arm blocked. The interferometric portion of both acquired photodetector array outputs for a single reflector in the sample arm is illustrated in Fig. 4 (a), and the corresponding Ascan from a single detector output is illustrated in Fig. 4 (b). The quadrature signal, obtained by using $\Delta\phi_{mn}$ and β_{mn} presented in Fig. 3 in Eq. (5), is plotted in Fig. 4 (c) and the complex conjugate resolved Ascan is shown in Fig. 4 (d). The data indicates a suppression of the complex conjugate peak of >20dB, and an SNR gain of ~5dB over that of the single detector. The small artifacts at DC and a ghost remnant of the negative image of the reflector observed in the conjugate resolved Ascan are likely due to slight mismatches in the spectrometer alignments. The peak height of the suppressed of the complex conjugate ambiguity is shown to be relatively constant as a function of depth in Fig. 5, and the peak SNR was measured as ~93dB.

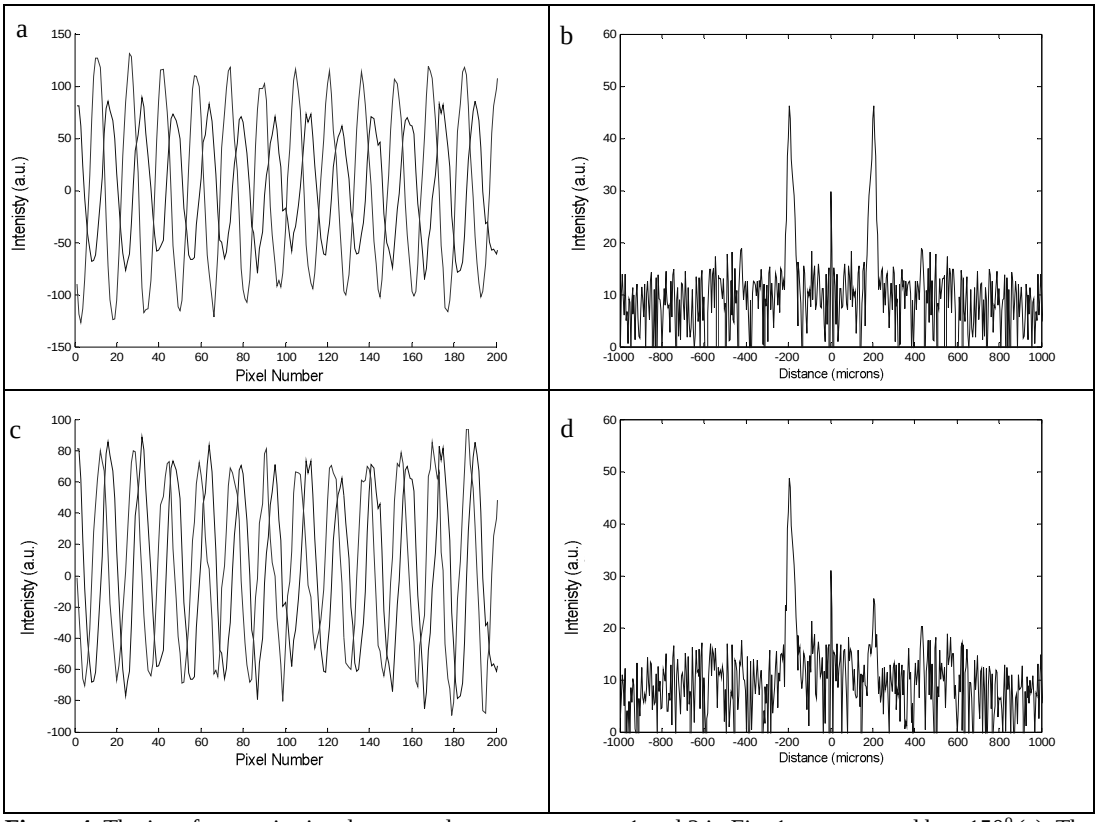

Figure 4. The interferometric signal measured on spectrometers 1 and 2 in Fig. 1 are separated by ~150^o (a). The Ascan obtained by Fourier transform of a single spectra (b) demonstrates the complex conjugate ambiguity and a DC artifact at zero displacement. (c) The real (0^o) and complex (90^o) components of the spectra derived from Eq. 5 are plotted. (d) The resulting A-scan obtained by Fourier transformation of the complex signal in (c) resolves the complex conjugate ambiguity, revealing the reflector position to the right of DC with small artifacts on the left side and at zero displacement.

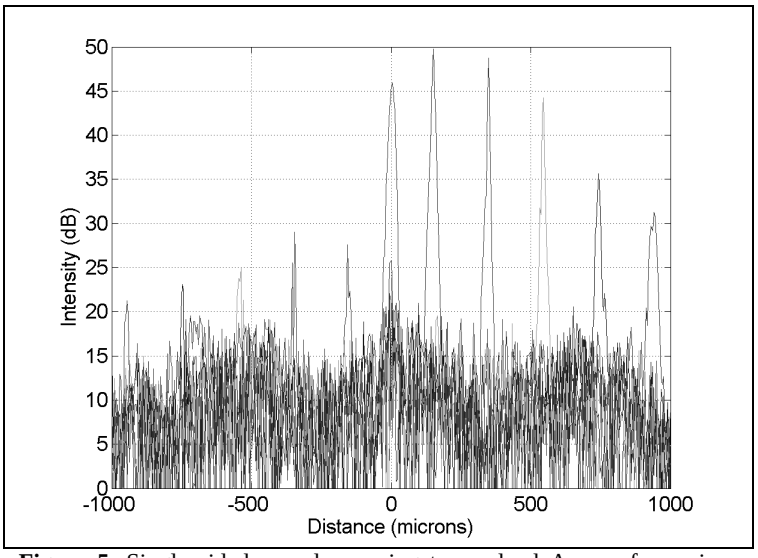

Figure 5. Single sided complex conjugate resolved Ascans for various path length differences. The peak SNR ~93dB, measured with 1mW on a mirror in the sample arm attenuated with a 2.5OD neutral density filter.

B-scans of a zebrafish eye are presented in Fig. 6. For both images, the DC spectrum was obtained by computing the average of all the collected spectra. The image on the left (Fig. 6(a)) was processed using only one of the two detector outputs. In this case, the complex conjugate ambiguity is not resolved and severe artifacts are observed. Using Eq. (5) to obtain both quadrature components and using the signal acquired simultaneously from both detector outputs demonstrates that the complex conjugate ambiguity has been resolved (Fig. 6 (b)). The ambiguity resolved image is clearly superior, with the exception of an artifact at DC arising from imperfect subtraction of the DC signal component.

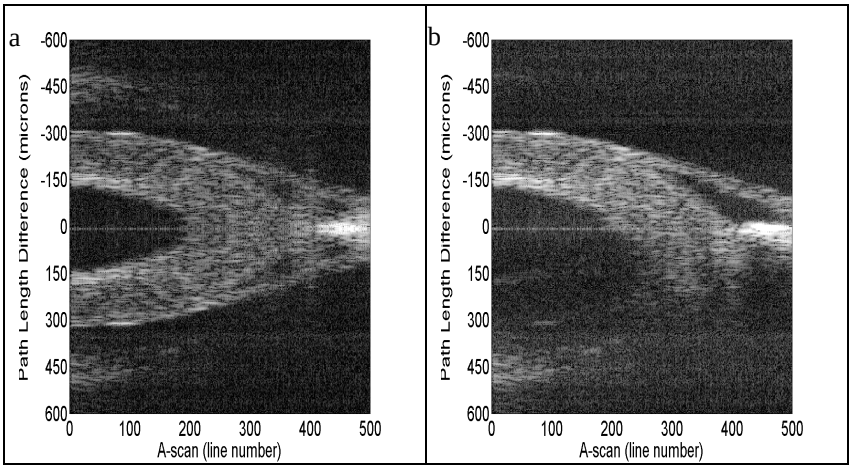

Figure 6. B-Scans of a plastic sheet using a 3x3 Michelson interferometer. In (a) only a single detector output was used to generate the A-scan, and the complex conjugate ambiguity is manifested as overlapping mirror images. (b) The full quadrature signal generated from the acquired spectra using Eq. 5 resolves the complex conjugate ambiguity, resulting in a clear image of the sample. The full depth of each A-scan is 1200μm; 500 A-scans were acquired spanning 0.5mm lateral displacement. Both images contain an artifact at zero displacement due to imperfect DC signal subtraction.

In summary, we have demonstrated that the complex conjugate ambiguity in SDOCT approaches may be removed by use of novel interferometer designs based on a 3x3 coupler.

4. ACKNOWLEDGEMENTS

Funding for this project was generously donated by the NIH grant #R24 EB00043.

REFERENCES

1. R. A. Leitgeb, C. K. Hitzenberger, and A. F. Fercher, *Performance of fourier domain vs. time domain optical coherence tomography*, Opt. Express, 2003.**11:** p. 889-894.
2. M. Choma, M.V. Sarunic, C. Yang, K. Hsu, and J.A. Izatt, *Sensitivity advantage of swept-source and Fourier-domain optical coherence tomography, SPIE Photonics West 2004, conference BO13,* submitted.
3. S. R. Chinn, E. A. Swanson, and J. G. Fujimoto, *Optical coherence tomography using a frequency-tunable optical source, Opt. Lett.* 22(5), 340-342 (1997).
4. M. Wojtkowski, A. Kowalczyk, R. Leitgeb, and A. F. Fercher, *Full range complex spectral optical coherence tomography technique in eye imaging, Opt. Lett.* **27**(16), 1415-1417 (2002).
5. M.A. Choma, C. Yang, and J.A. Izatt, *Instantaneous Quadrature Low Coherence Interferometry With 3x3 Fiber Optic Couplers, Opt. Lett.*, submitted, 2003. Also presented as a post-deadline paper at CLEO 2004.
6. Breguet, J. and N. Gisin, *Interferometer using a 3x3 coupler and Faraday mirrors.* Optics Letters, 1995. **20**(12): p. 1447-1449.
7. ANSI, *American National Standard for Safe Use of Lasers, ANSI Z 136.1-1993*. 1993, Orlando, Fla: The Laser Institute of America. 37-43.